Effect of mixed Frenkel and charge transfer states in time-gated fluorescence spectra of perylene bisimides H-aggregates: Hierarchical equations of motion approach

Effect of Frenkel and Charge transfer mixing states on the exciton delocalization in PBI H-aggregates. Ultrafast dynamics employing the HEOM approach.

(Dated: 21 May 2022)

We theoretically investigate the effect of the mixing Frenkel (F) and charge transfer (CT) states in the dynamics and spectral properties of perylene bisimides (PBI) derivatives, focusing on Me-PTCDI due to the strong interaction via electron transfer. The model consists of a four-level system described by the Holstein Hamiltonian coupled to independent local heat baths for each site, described by Brownian spectral distribution functions. We employ the reduced hierarchy equations of motion (HEOM) approach to calculate the time evolution of the system as a function of the F-CT transfer integrals and compare it to the oligomer cases. We compute the absorption and time gated fluorescence (TGF) spectrum for different conditions of exciton and CT transfer integrals and F-CT band gap. We then compute the coherence length (N_{coh}) employing the theoretical definition and the graphical approximation. We observe the presence of an excited hot peak which intesity related to the grade of delocalization and ultrafast dymanics that are solely dependent on the frequency of the local bath. The results indicate that the inclusion of CT states promote localization of the excitons which is manifested in the decrease in the intensity of the hot peak and increase of the 0-0 emision band in the TGF spectrum, leading to a decrease in the coherence length.

I. INTRODUCTION

In the past couple of decades, the development of more efficient photovoltaic devices has been a topic of great interest in the investigation of renewable energy sources. In particular, organic solar cells have shown to be promising materials because of its low fabrication cost, lightweight and the flexibility of design in comparison to silicon-based materials exist in the market.[1,2]. Consequently, several groups have been studying different types of compounds that could be used as donor and acceptors (such as oligoacenes and fullerene/non-fullerene derivatives, respectively)[3], to increase the power conversion efficiency. In this direction, perylene bisimides (PBI) derivatives are conjugated molecules with a tendency to form $\pi - \pi$ stacked H-aggregates that have shown to have remarkable photostability and exhibit different spectral properties such as change of color based on the substituent employed, making it promising candidates for the possible applications as semiconductors.[4,5]

The mechanism involved in the photocurrent generation in organic devices is more complicated in comparison to the inorganic counterparts, mainly because of the vibronic effects associated to a strong electron-phonon interaction. Recently, the importance of the inclusion of charge transfer (CT) states and the interaction with Frenkel (F) states on the exciton dynamics of certain systems have been pointed out (ref). Particularly, in systems where this interaction is strong, the Frenkel approximation is not enough to accurately reproduce certain optical properties. Thus, in order to improve the efficiency of such systems, quantum coherence effects between the electron and phonon plays an essential role and methods that allow a quantum mechanical description of system-bath interaction have to be employed to effectively describe the dynamics, specially at ultrafast time scales.[6] Some studies have reported that localization processes can efectively occur on these ultrafast time scales, competing with the energy transfer processes (ref), but to our knowledge, experimental results could not be obtained yet due to technological limitations. The number of theoretical studies related to this topic are scarse and, furthermore, analysis of this type of systems employing numerical exact methods such as the Hierarchy Equations of Motion (HEOM) have not been yet found in the bibliography.

The absorption and photoluminescence (PL) spectrums can provide information regarding the nature of the electronic excitations, such as the effect of aggregation, vibronic coupling and the effect on the spatial coherence.Some of the characteristic behaviour of J- and H-aggregates absorption and emission spectrums with the vibronic coupling have been previouly reported in the literature and compared with the single molecule spectrum (ref) . The spatial coherence is of particular importance because it is directly related to energy transfer and determines electronic correlation between molecular sites in a delocalized excited state. In this direction, the coherence lenght (N_{coh}) is a widely employed parameter to calculate the grade of delocalization of excitons and, recently, a method was proposed to determine it through experiment by calculating the 0-0 to 0-1 fluorescence peak ratio (ref). This method is currently assumed to accurately reproduce the values of N_{coh} for J- aggregates, but for H-aggregates is assumed to work only in the short times due to the "inversion" of the 0-0 and 0-1 peak intensities. Femtosecond time-gated fluorescense (TGF) measurements can be performed experimentally for PBI H-aggregates in the excited state in order to study the exciton coherence (ref). However, the limitations of the time gate available to obtain the TGF spectrum makes difficult to analyze the behaviour of the exciton dynamics at shorter times (ultrafast dynamics) which may be important. On the other hand, the TGF spectrum can be obtained theoretically by employing the HEOM formalism for any given time gate and used to give and insight of the behaviour at ultrafast times and the impact on the N_{coh} behaviour in relation to the experimental approximation.

In order to study electron transfer problems in connection to open quantum dynamics theory, a commonly used model considers the electronic states coupled to an intermediate harmonic oscillator, which is further coupled to a heat bath.[7]

Then, the harmonic mode can be included in the bath by carrying out a canonical transformation, which leads to a multilevel system coupled to the heat bath with the Brownian spectral distribution (BSD) function.[8] Such a system can be treated using the HEOM formalism, in a numerically rigorous manner,[9] even in the low temperature case. The HEOM formalism can handle not only the strong system-bath coupling but also quantum coherence between the system and bath that is important for the investigation of the organic materials.[10,11].

In this paper, we present a study of the influence of CT states in the dynamics and spectral properties of PBI aggregates, using Me-PTCDI (N,N'-dimethyl-3,4,9,10-perylenetetracarboxylic diimide) as a reference due to its particularly strong F-CT interaction via electron transfer integral. We employ the HEOM approach for a BSD function to simulate the non-Markovian dynamics and the optical properties of the Holstein model that is further coupled to the heat-bath.

The organization of this paper is as follows: In Sec. II A, we present the equations for the Holstein Hamiltonian in the present system using the Hierarchy equations of Motion, the equations for the calculation of the absorption and emission spectrums and the definition of the coherence lenght (N_{coh}). Then, the model system is explained. In Sec. III we present the details of the calculation and the results of the simulation for various conditions. Sec. IV is devoted to concluding remarks.

II. THEORY

A. The HEOM for a Holstein + bath system

The HEOM for a Holstein-Pierls Hamiltonian was introduced in a previous work (ref). For this particular system, we consider the main contribution of the bath to be the linearly coupled local (Holstein) interactions of the electronic system with an optical phonon mode at each site, which are further coupled to a harmonic oscillator heat-bath.

The total Hamiltonian is expressed in terms of the electronic Hamiltonian ($\hat{H}_{el}$), the electron-phonon interaction Hamiltonian ($\hat{H}_{el-ph}$) and the local phonon mode interaction with the heat-bath ($\hat{H}_{ph-B}$) as

$$\hat{H}_{tot} = \hat{H}_{el} + \hat{H}_{el-ph} + \hat{H}_{ph-B}, \tag{1}$$

Following the procedure of Gisslén et al., the electronic hamiltonian is then divided in terms of the contribution of Frenkel states (F), Charge Transfer (CT) states and the interaction between the two of them (F-CT). (ref)

$$\hat{H}_{el} = \hat{H}_F + \hat{H}_{CT} + \hat{H}_{F-CT}, \tag{2}$$

where each term is expresed as

$$\hat{H}_F = \sum_i \varepsilon_i^0 \hat{a}_i^\dagger \hat{a}_i + \sum_{i\neq j} t_{ij}^0 \hat{a}_i^\dagger \hat{a}_j \tag{3}$$

$$\hat{H}_{CT} = \sum_m \varepsilon_m^0 \hat{a}_m^\dagger \hat{a}_m + \sum_{m\neq n} t_{mn}^0 \hat{a}_m^\dagger \hat{a}_n \tag{4}$$

$$\hat{H}_{F-CT} = \sum_{mn\neq ij} t_{mn,ij}^0 \hat{a}_{mn}^\dagger \hat{a}_{ij}, \tag{5}$$

The electron-phonon interaction Hamiltonian is

$$\hat{H}_{el-ph} = \sum_i \sum_\alpha \hat{V}_\alpha^i \left(\hat{b}_\alpha^\dagger + \hat{b}_\alpha\right) + \sum_m \sum_\alpha \hat{V}_\alpha^m \left(\hat{b}_\alpha^\dagger + \hat{b}_\alpha\right), \tag{6}$$

with

$$\hat{V}_\alpha^i = \frac{1}{\sqrt{\mathscr{N}_C}} \hbar\Omega_\alpha g_i^\alpha \hat{a}_i^\dagger \hat{a}_i,$$
$$\hat{V}_\alpha^m = \frac{1}{\sqrt{\mathscr{N}_C}} \hbar\Omega_\alpha g_m^\alpha \hat{a}_m^\dagger \hat{a}_m,$$

Finally, the phonon-bath Hamiltonian is expresed as

$$\hat{H}_{ph-B} = \sum_\alpha \hbar\Omega_\alpha \left(\hat{b}_\alpha^\dagger \hat{b}_\alpha + \frac{1}{2}\right) + \sum_\alpha \sum_{k=1}^{N_\alpha} \hbar\omega_k \left(\hat{b}_k^\dagger \hat{b}_k + \frac{1}{2}\right) + \sum_\alpha \left(\hat{b}_\alpha^\dagger + \hat{b}_\alpha\right) \sum_{k=1}^{N_\alpha} c_k^\alpha \left(\hat{b}_k^\dagger + \hat{b}_k\right). \tag{7}$$

Here, $\hat{a}_i^\dagger$ ($\hat{a}_m^\dagger$) and $\hat{a}_i$ ($\hat{a}_m$) are the creation and annihilation operators, respectively, of the Frenkel excitons (Charge Transfer) states. Moreover, ε_i^0 (ε_m^0) and t_{ij}^0 (t_{mn}^0) are the on-site electronic energy and the ampliture of the transfer integral for the $i-j$th Frenkel states ($m-nth$ Charge Transfer states). The term $t_{mn,ij}^0$ represents the tranfer parameter between Frenkel and Charge Transfer states with $\hat{a}_{mn}^\dagger$ and $\hat{a}_{ij}$ being the creation and annihilation operator of the respectively states. The creation (annihilation) operator of the phonon (or vibron) mode α with the frequency Ω_α is expressed as $\hat{b}_\alpha^\dagger$ ($\hat{b}_\alpha$) . The local system-bath interactions are expressed as $\hat{V}_\alpha^i$ and $\hat{V}_\alpha^m$ for the Frenkel and Charge Transfer terms, with the dimensionless coupling strength g_i^α and g_m^α, respectively. The constant $\mathscr{N}_C$ is the number of unitary cells considered. The operator $\hat{b}_k^\dagger$ ($\hat{b}_k$) is the creation (annihilation) operator of the heat-bath that can be characterized by the oscillator-bath coupling strength and the inverse temperature $\beta \equiv 1/k_B T$, where k_B is the Boltzmann constant. The bath system is typically modeled by the spectral distribution function (SDF), defined by

$$J_\alpha(\omega) \equiv \sum_\alpha \sum_{k=1}^{N_\alpha} (c_k^\alpha)^2 \, \delta(\omega - \omega_k). \tag{8}$$

For the heat bath to be an unlimited heat source possessing an infinite heat capacity, the number of heat bath oscillators N_α is effectively made infinitely large by replacing $J_\alpha(\omega)$ with a continuous distribution.

By using the canonical transformation, the Hamiltonian in Eq.(1) can be expressed in terms of the creation and annihilation operators of the heat-bath + primary oscillation ($\hat{b}_k'^\dagger$ and $\hat{b}_k'$, respectively) in the following general form

$$\hat{H}_{tot} = \hat{H}_{el} + \sum_\alpha \sum_{k=1}^{N_\alpha} \sum_i d_k^{ii\alpha} \hat{a}_i^\dagger \hat{a}_i (\hat{b}_k'^\dagger + \hat{b}_k') + \sum_\alpha \sum_{k=1}^{N_\alpha} \hbar\omega_k \left(\hat{b}_k'^\dagger \hat{b}_k' + \frac{1}{2}\right), \tag{9}$$

where $d_k^{ii\alpha}$ is the dimensionless constant that represent the local interaction of the system with the oscillator-bath. Assuming that the SDF of the later to be $J_\alpha(\omega) = \gamma_\alpha \omega$, we have the

BSD defined as

$$J'_\alpha(\omega) = \frac{\hbar\lambda_\alpha}{2\pi}\frac{\gamma_\alpha\Omega_\alpha^2\omega}{(\Omega_\alpha^2-\omega^2)^2+\gamma^2\omega^2}, \tag{10}$$

where λ_α relates to the reorganization energy which accounts for the displacement of the excited state in a relation to the ground state in coordinate space as a consequence of the local electron-phonon interaction. The parameter γ_α is the coupling strength between the oscillator and the bath, which is related to the peak width of $J'_\alpha(\omega)$.

The reduced hierarchy equations of motion for the Brownian distribution can be expressed as

$$\begin{aligned}\frac{\partial}{\partial t}\hat{\rho}_{\{n^\alpha,m^\alpha;j_1^\alpha\cdots j_K^\alpha\}}(t) = &-\left[\frac{i}{\hbar}\hat{H}_{el}^{\times}+\sum_\alpha\left\{\frac{(n^\alpha+m^\alpha)}{2}\gamma_\alpha - i(n^\alpha-m^\alpha)\zeta_\alpha+\sum_{k=1}^{K^\alpha}j_k^\alpha\nu_k^\alpha-\hat{\Xi}_\alpha\right\}\right]\hat{\rho}_{\{n^\alpha,m^\alpha;j_1^\alpha\cdots j_K^\alpha\}}(t)\\
&+\sum_\alpha\hat{V}_\alpha^{\times}\left[\hat{\rho}_{\{n^\alpha+1,m^\alpha;j_1^\alpha\cdots j_K^\alpha\}}(t)+\hat{\rho}_{\{n^\alpha,m^\alpha+1;j_1^\alpha\cdots j_K^\alpha\}}(t)\right]\\
&+\sum_\alpha n^\alpha\hat{\Theta}_-^\alpha\hat{\rho}_{\{n^\alpha-1,m^\alpha;j_1^\alpha\cdots j_K^\alpha\}}(t)+\sum_\alpha m^\alpha\hat{\Theta}_+^\alpha\hat{\rho}_{\{n^\alpha,m^\alpha-1;j_1^\alpha\cdots j_K^\alpha\}}(t)\\
&+\sum_\alpha\sum_{k=1}^{K^\alpha}\hat{V}_\alpha^{\times}\hat{\rho}_{\{n^\alpha,m^\alpha;j_1^\alpha\cdots j_{k+1}^\alpha,\cdots j_K^\alpha\}}(t)+\sum_\alpha\sum_{k=1}^{K^\alpha}j_k^\alpha\nu_k^\alpha\hat{\Psi}_k^\alpha\hat{\rho}_{\{n^\alpha,m^\alpha;j_1^\alpha\cdots j_{k-1}^\alpha,\cdots j_K^\alpha\}}(t),\end{aligned} \tag{11}$$

where the first term in brackets is the Liouvillian ($\hat{\mathscr{L}}^{(n,m)}$) that involves the temperature correction terms. For a high number of hierarchy elements, the term $(n^\alpha+m^\alpha)\gamma_\alpha/2+\sum_{k=1}^{K^\alpha}j_k^\alpha\nu_k^\alpha$ becomes much larger than the characteristic time of the system. In this case, the hierarchy can be truncated by the terminator.[12]

B. Absorption and Emission spectrum

In optical measurements, the physical obserbables are related to the response function which describes the interaction of the incoming radiation or pulses $\hat{\mu}$ with the system represented by the density matrix $\hat{\rho}_{tot}(t)$. Linear absorption is related to the first order response function expanded in terms of the laser interaction as

$$\hat{R}^{(1)}(t_1) = \frac{i}{\hbar}\left\langle\left[\hat{\mu}(t_1),\hat{\mu}(0)\right]\right\rangle \tag{12}$$

$$= \frac{i}{\hbar}Tr\left\{\hat{\mu}e^{-i\hat{L}_{tot}^0 t_1}\hat{\mu}^{\times}\hat{\rho}_{tot}^{eq}\right\}, \tag{13}$$

Here, ρ_{tot}^{eq} is the initial equilibrium state of the system and $\hat{L}_{tot}^0$ is the Liouvillian operator of the system without the laser interaction. The evolution of the density matrix elements after the pulse can be computed directly employing the HEOM formalism described in the previous section. The intensity of the signal corresponding to the absortion spectrum then is obtained by performing the Fourier transform of the response function.

$$I_{Abs}(\omega) = Im\int_0^\infty dt R^{(1)}(t_1)e^{i\omega t}, \tag{14}$$

The third order response function is associated with nonlinear optical processes and is calculated for a time ordered of four pulse secuences as follows

$$\hat{R}^{(3)}(t_3,t_2,t_1) \tag{15}$$

$$= \frac{i}{\hbar^3}\left\langle\left[\left[\left[\hat{\mu}(t_1+t_2+t_3),\hat{\mu}(t_1+t_2)\right],\hat{\mu}(t_1)\right],\hat{\mu}(0)\right]\right\rangle \tag{16}$$

$$= \frac{i}{\hbar^3}Tr\left\{\hat{\mu}e^{-i\hat{L}_{tot}^0 t_3}\hat{\mu}^{\times}e^{-i\hat{L}_{tot}^0 t_2}\hat{\mu}^{\times}e^{-i\hat{L}_{tot}^0 t_1}\hat{\mu}^{\times}\hat{\rho}_{tot}^{eq}\right\}, \tag{17}$$

The design of the pulse sequency is what will determine the shape of the response function which can be associated to a specific spectroscopical technique. The first pulse creates a coherence during the t_1 period and the second pulse creates an optical excitation of the system. If we assume instant excitation, i.e $t_1 = 0$, one can neglect resonant Raman scattering contributions. We can then compute the time gated fluorescense signal (TGF) which is associated to the spontaneous emision (SE) signal at different times (t^*) as follows

$$S_{SE}(t^*,\omega) = Re\int_0^\infty dt_3\int_0^\infty dt_2 R^{(3)}(t_3,t_2,0)E_G(t_2-t^*) \tag{18}$$

$$\times E_G(t_2+t_3-t^*)e^{i\omega t_3}, \tag{19}$$

where E_G represents the amplitude of the time-gate pulse. Thus, to obstain the third order response function, we can calculate the population dynamics at times t_2 and then the first order response function at times t_3 for each t_2. The TGF signal is then obtained by performing the Fourier transform including the time-gate pulse.

C. Coherence Lenght

The coherence lenght (N_{coh}) is a widely employed parameter to calculate the grade of delocalization of excitons. During the years, several deffinitions have been introduced, but here we employ two of them. The first one is associated with the

autocorrelation function (ref) and thus, with the density matrix elements and can be directly computed from the dynamics of the system as

$$N_{coh}(t) = \frac{1}{|C(t,0)|}\sum_{s}|C(t,i)| \tag{20}$$

$$C(t,i) = Tr\left[\sum_{i,j}\hat{a}_i^{\dagger}\hat{a}_j\rho^{(2)}(t,0)\right], \tag{21}$$

where C(t,i) is called the coherence field, which depends on the $i-th$ site and $\rho^{(2)}(t,0)$ is the on site density matrix after the two laser excitations. The second method was described by Spano et al. as a relation between the intensities of the 0-0 and the 0-1 emssion bands and it's used as an approximation (ref).

$$N_{coh}(t^*) \approx \lambda^2\frac{I^{0-0}(t^*)}{I^{0-1}(t^*)}, \tag{22}$$

where the intensities can be directly obtained from the TGF spectrum and λ^2 is the Huang-Rhys factor.

III. RESULTS AND DISCUSSION

We chose Me-PTCDI as a reference molecule under study due to the strong reported values of the transfer integrals related to the charge transfer states (ref).In order to simulate the exciton transfer process between the molecules, we consider a four-level system to model a dimer in which the first two components correspond to the F states and the last two correspond to the CT states of each molecule, respectively. For comparison purposes, we also include calculations of the monomer, dimer and tetramer.

Thus, the system is described by two F states and two CT states expressed as $|1\rangle$, $|2\rangle$, and $|3\rangle$, $|4\rangle$, respectively (illustrated in Fig. 1). In this model, each state is coupled to its own local vibrational mode, which is further coupled to the heat-bath. We consider the frequency and the coupling strenght of the vibrational modes to be identical for the two F states, but different coupling strenghts for the two CT states. We also consider that there is no transfer between CT states. For the case of the dimer and tetramer, the system consists only of F states and we assume the transfer parameters to be restricted to the nearest neightbour condition.

The electronic Hamiltonian is then expressed in the matrix form as

$$\hat{H}_{el} = \hbar\begin{bmatrix}\omega_1 & \Delta_{12} & \Delta_e & \Delta_h\\ \Delta_{21} & \omega_2 & \Delta_h & \Delta_e\\ \Delta_e & \Delta_h & \omega_3 & 0\\ \Delta_h & \Delta_e & 0 & \omega_4\end{bmatrix}, \tag{23}$$

where $\hbar\omega_i$ is the F exciton (CT) energy of the ith (mth) state assosiated with ε_i (ε_m) and $\hbar\Delta_{ij}$ ($\hbar\Delta_{ij}$) is the coupling strength between the ith and jth (mth and nth) states assosiated with the transfer integral t_{ij} (t_{mn}). For all of our computations, we fixed

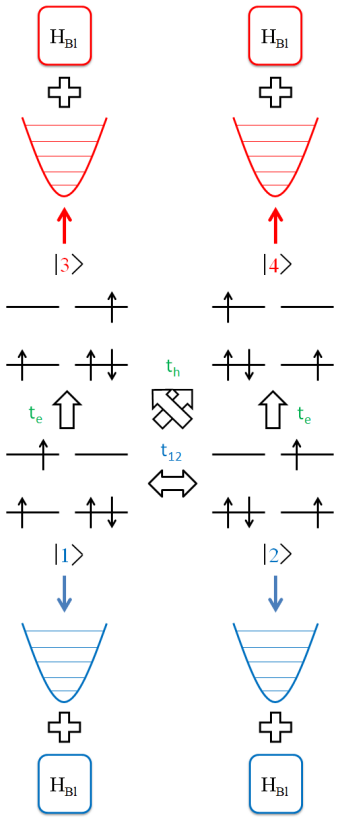

FIG. 1. Schematic view of the model that is described by the Hamiltonian given in Eqs.(1)-(7) for the Frenkel + Charge Transfer states four level system. Each state is coupled to its own local vibrational mode and to the local bath (H_{Bl}).

the eigenenergy of the F states as $\omega_1 = \omega_2 = 0cm^{-1}$ and consider the room temperature case ($T = 300$K) with the value of $\beta\hbar\omega = 2.40$. Although we analyze the effect of the energy band gap between F and CT states, we initially consider the eigenenergy of the CT states to be $\omega_3 = \omega_4 = 480\text{cm}^{-1}$. The off-diagonal elements representing the interaction between excited states are $\Delta_{12} = \Delta_{21} = 500cm^{-1}$. For the F-CT interaction parameters, we set the electron transfer integrals to $\Delta_e = -725cm^{-1}$ and the hole transfer integrals to $\Delta_h = -160cm^{-1}$. As mentioned before, we consider no transfer between CT states and set their transfer terms to $0cm^{-1}$.

The system-bath interaction for each one of the states is independent and thus we consider four vibrational modes. The F and CT states are coupled to the main vibrational mode of frequency $\Omega_1 = \Omega_2 = \Omega_3 = \Omega_4 = 1400cm^{-1}$ with coupling strength $\lambda_1 = \lambda_2 = 1200cm^{-1}$, $\lambda_3 = 850cm^{-1}$ and $\lambda_4 = 465cm^{-1}$. The coupling strength between the local oscillator and the bath, which acts as the inverse noise correlation time of the BSD, is fixed to $\gamma = 500cm^{-1}$. The initial condition of the system at $t = 0$ is set by $\rho_{11}(0) = 1$ and $\rho_{22}(0) = \rho_{33}(0) = \rho_{44}(0) = 0$. We simulate the time evolution of the reduced density matrix by numerically integrating the HEOM with respect to the time using the fourth-order Runge-Kutta method. The depth and the truncation number of hierarchy are chosen to $N = 10$ with $K = 2$.

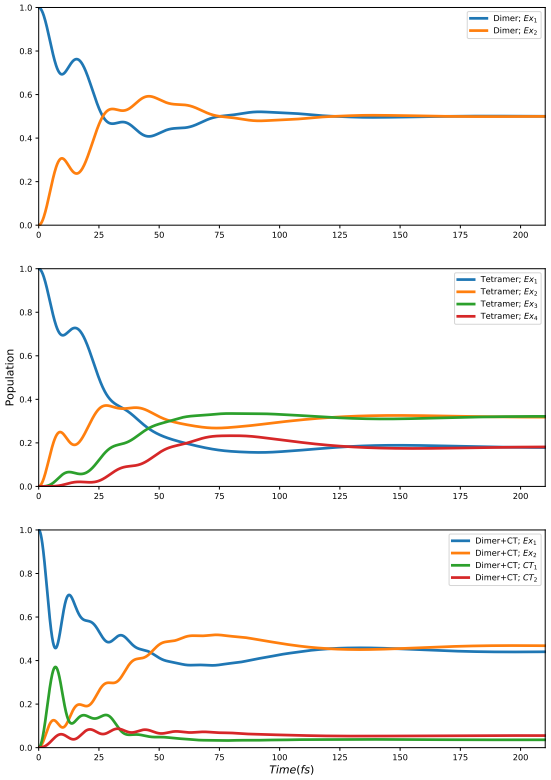

FIG. 2. Time evolution of the density matrix elements for the dimer, tetramer and dimer+CT states.

.

The time-evolution of the reduced density matrix for the dimer, tetramer and dimer+CT state is shown in Fig. 2. The dynamics are calculated up to a time of $t = 210fs$ which is enough to reach equilibrium on this conditions. We can observe an ultrafast process in the range of 50fs followed by thermalization. Looking at the CT dynamics, there is a substantial increase in the population of state $|3\rangle$ at shorter times and an inversion in the population rate with $|4\rangle$ at longer times. This happens because the absolute value of the electron transfer integral between $|1\rangle$ and $|3\rangle$ is almost 5 times larger than the value of the hole transfer integral between $|1\rangle$ and $|4\rangle$, thus allowing faster exchange between the formers at shorter times. However, the coupling with the local vibrational mode is around 2 times larger for $|3\rangle$ than $|4\rangle$ which means that the relaxation in stronger at longer times, which produces the inversion of the populations. The effect of changing the electron and hole transfer integral parameters is shown in Fig.S1 (Suplementary) In general, when increasing the transfer integrals, we can observe an increase in the population exchange of the CT state at shorter times and a slightly increase in the overall

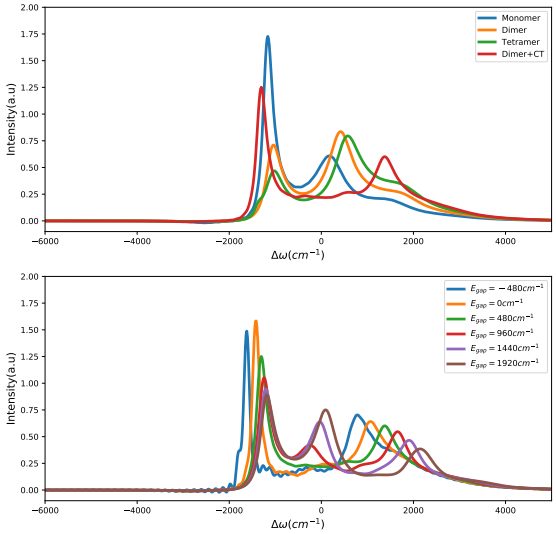

FIG. 3. Absorption spectrum for the monomer, dimer, tetramer and dimer+CT states (top) and absorption spectrum for the dimer+CT state system with different values of the energy band gap (E_{gap}) between Frenkel and CT states (bottom)

.

CT populations at equilibrium. Note that for this system, we chose a high value of γ in order to reproduce the bandwidth in the spectrums and also save computational time, which results in a fast relaxation of the system. The experimental relaxation time of this systems, however, have been reported on the order of 1ps. Thus, we assume that the actual value of γ is much smaller and that the broadening of the experimental spectrum could be associated to static disorder instead of the bath influence.

The absorption spectrum for the monomer, dimer, tetramer and dimer+CT state are illustrated in Fig. 3 (top). We can observe the A^1 main peak at frequencies around $-1200cm^{-1}$ and the A^2 and A^3 peaks for the monomer, dimer and tetramer. The difference in frequency between the peaks for the monomer correspond to the value of the local oscillator ($1400cm^{-1}$), which increases for the dimer and tetramer due to the effect of the transfer integral. We also observe an overall blue-shift of the spectrum when we increase the number of sites, together with a decrease in the intensity of the A^1 peak and an increase of the A^2 intensity, which is the expected behaviour for oligomers and was attributed to the $\pi-\pi$ stacking of PBIs molecules in H-aggregates (Shao et al.). (ref) For the dimer+CT, however, we observe that the A^1 peak is redshifted and more intense with respect to the isolated dimer and a second peak at frequencies around $1500cm^{-1}$. N. J. Hestand and F. C. Spano attributed the high frequency peak to the influence of the CT states. (ref) The absorption spectrum of the dimer and the spectrum due to the CT states are actually superposed and the distance between the main peak and

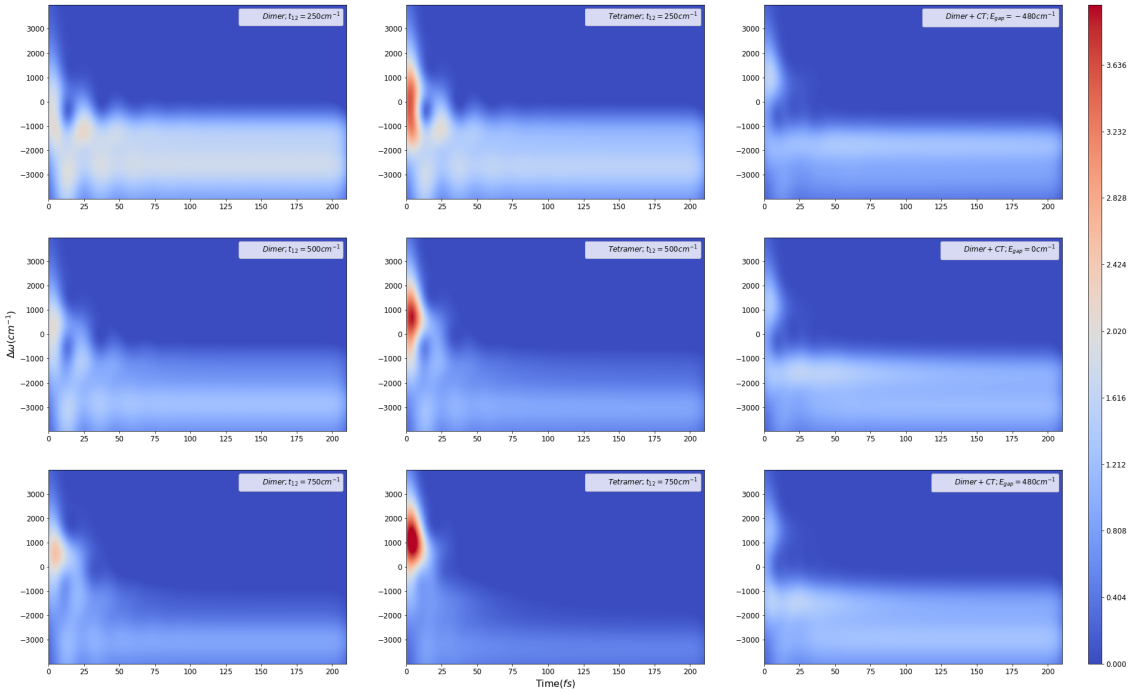

FIG. 4. TFG spectrum (time gate $t_G = 10fs$) of the dimer and tetramer for different values of the transfer integral (t_{12}) and of the dimer+CT states for different values of the energy band gap (E_{gap}) between Frenkel and Charge Transfer states

.

the high frequency peak was related to the effect of the electron and hole transfer integrals, which produces the split and the overall red-shift of the dimer part of the spectrum. The absorption spectrum for different values of electron and hole transfer integrals is shown in Fig. S2 (suplementary), where we can that the shift increases, the intensity of the A^1 peak increases and the intensity of the A^2 peak decreases when the overall CT transfer integral parameters increase. The effect of the band gap, on the other hand, was also reported by Hestand et al. and it's illustrated in Fig. 3 (bottom) for this system. (ref) When the band gap between the Frenkel and CT states is increased, the intensity of the A^1 peak and the high frequency peak slowly decreases. We can also observe that the A_2 peak increase in intensity and that there is an overall blue-shift of the spectrum. This is expected to happen, the spectrum tends to the spectrum of the dimer when the energy of the band gap increases to infinity.

The TGF spectrum of the dimer and tetramer for different values of the transfer integral (t_{12}) and of the dimer+CT states for different values of the energy band gap (E_{gap}) between Frenkel and Charge Transfer states is shown in Fig. 4 for a time gate $t_G = 10fs$. We can identify the 0-0 and 0-1 emission peaks in the dimer at approximately -1200^{-1} and $-2600cm^{-1}$, respectively, althought the displacement and the splitting increases with the number of sites and with higher values of the tranfer integral t_{12}. Furthermore, we observe a peak at possitive frequencies whose intensity and location increases under the same conditions. We assume that this peak is related to the presence of hot states after initial photoexcitation. Including CT states seems to supress this effect, manifested by the decrease in the intensity of the peak. The possition of the hot peak is also blue-shifted with increasing t_{12} and E_{gap} as a consequence of the increase splitting with the emission peaks, which is a similar behaviour to the one observed for the absorption spectrum and attributed to the molecular stacking. The results obtained for the oligomers for a time gate of $t_G = 50fs$ are illustrated in Fig.S3 (suplementary) and are similar to those reported in the bibliography (Sung et al.), although for a different derivative.

During the time evolution, we can observe the dynamics of the wavepacked due to the short time-gate employed. The initial intensity of the 0-0 emission is weaker and decays faster with increasing values of t_{12} and E_{gap}. We can see an initial ultrafast localization before reaching equilibrium in the order of the first 50fs. We assume that this is due to an initial relaxation of the hot Frenkel excited states resulting from the interaction with the bath, followed by the transfer over the molecular sites. We can clearly see the movement of the wavepacked

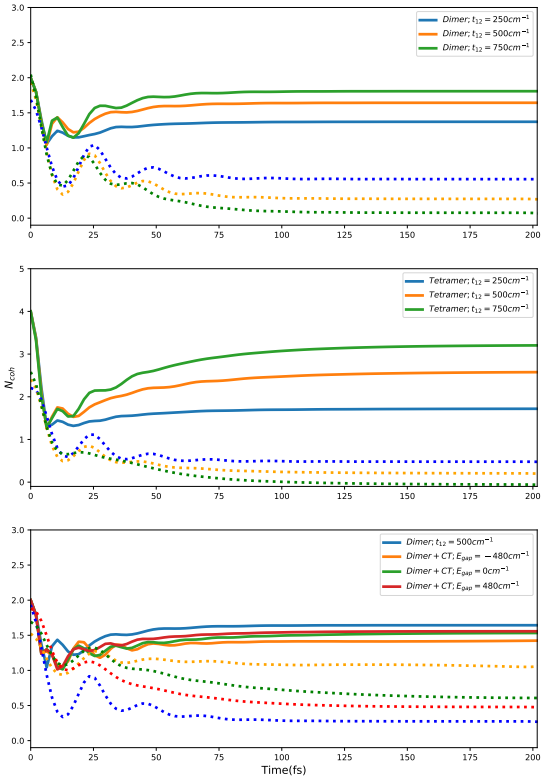

FIG. 5. Estimation of the coherence lenght (N_{coh}) using the theoretical definition (color lines) and the graphical approximation (dotted lines) for the dimer and tetramer for different values of the transfer integral (t_{12}) and for the dimer+CT states for different values of the energy band gap (E_{gap}) between Frenkel and Charge Transfer states

.

from the initially excited hot state to the 0-0 emission band, followed by the transfer to the 0-1 emission band. The dynamic oscillation is directly associated to the frequency of the heat bath, which has a time period of $1/\Omega = 24fs$ and is independent of other system/bath parameters. A decrease in the 0-0 emission peak in relation to the 0-1 emission was related to an increase in the grade of delocalization in H-aggregates and associated to the coherence lenght N_{coh} defined in Eq.(21).

The time evolution of N_{coh} for all the previous conditions is shown in (Fig. 5) for both the theoretical definition (color lines) and the graphical approximation (dotted lines). We observe that, for the results obtained using Eq.(21), the equilibrium value increase with increasing t_{12} and E_{gap} as expected. We can also observe the ultrafast dynamics and the initial localization before reaching equilibrium. The inclusion of the CT states, then, seems to promote localization of the excitons which is manifested in several results such as the increase of the intensity of the A^1 peak and decrease of the A^2 in the absorption spectrum; and the decrease in the intensity of the hot band and increase of the 0-0 emision band in the TGF spectrum, leading to a decrease in the coherence length. In some works, the effect of the CT states were described as an intermediate mechanism between exciton delocalization and excimer formation (ref). The results obtained employing the approximation of Eq.(22), on the other hand, are notably different in comparison to the analytical calculation. The coherence leght goes to a value lower than 1 at longer times which is a problem that arises when using this approximation as previously stated (ref). Note that in this approximation, the coherence length is calculated for a specific time gate, thus the vibrational effects at shorter times can only be seen for small enough values of t_G, which might be a problem due to the experimental the lower limit being aroud 50fs. This behaviour is shown in Fig.S4 (suplementary) for different time gates where we can clearly see how the ultrafast dynamics vanish at longer time gates. Another important point is that the values of N_{coh} at equilibrium for different transfer integral parameters should increase (increase delocalization) when t_{12} increases (as showed in the analitical results), however we see the opposite behaviour due to the inversion in the intensities of the peaks in H-aggregates. We conclude that this approximation is not adecuate to accurately compute N_{coh} for H-aggregates. It was reported in the bibliography that the approximation works well for J-aggregates. Because we are only computing results for a H-aggregate system, we can not confirm nor deny this statement at present, but the accuracy problem at ultrafast times may remain if long time gates are used.

IV. CONCLUSION

We employed the HEOM approach for a Holstein hamiltonian to study the effect of mixing F-CT states in PBI H-aggregates. We evaluated the dynamics and spectral properties of Me-PTCDI for different exciton and CT conditions in order to understand the influence in the exciton delocalization.

The obtained absorption spectrums and some of their behaviour are in agreement with previously reported studies. Some of the effects when considering CT states include the red-shift and increase in intensity of the A^1 peak with respect to the isolated dimer, the decrese in intensity of the A_2 peak and the appearence of a higher frequency peak as a consequence of the splitting due to the F-CT interaction.

The calculation of the TGF allowed us to see the presence of ultrafast dymanics that are solely dependent on the frequency of the local bath and are currently not possible to obtain experimentally due to technological limitations. We observed the presence of an excited hot peak which intesity is related to the grade of delocalization and its decay time is four to five times shorter than the relaxation of the system. The inclusion of CT states showed to has a major impact during the ultrafast dynamics, which was later shown in the decrease of the hot peak and increase of the 0-0 emision peak on the TGF spectrum. These results indicated that CT states promote localization of the excitons, which was manifested in a decrease

in the coherence length. On the other hand, the discrepancies observed when computing N_{coh} using the graphical approximation were rather high and thus we suggest caution when employing it in the case of H-aggregates.

ACKNOWLEDGMENTS

The financial support from The Kyoto University Foundation is acknowledged. M.C. is supported by the Japanese Government (MEXT) Postgraduate Scholarships.

DATA AVAILABILITY

The data that support the findings of this study are available from the corresponding author upon reasonable request.

[1] G. Horowitz, "Organic field-effect transistors," Adv. Mater. **10**, 365–377 (1998).
[2] C. D. Dimitrakopoulos and P. R. L. Malenfant, "Organic thin film transistors for large area electronics," Adv. Mater. **14**, 99–117 (2002).
[3] J. Zhang, H. S. Tan, X. Guo, A. Facchetti, and H. Yan., "Material insights and challenges for non-fullerene organic solar cells based on small molecular acceptors," Nature Energy **3**, 720–731 (2018).
[4] K. Sato and J. Mizuguchi, "Crystal structure of parallel-stacked peryleneimides and their application to organic field-effect transistor devices," J. Appl. Phys. **103**, 013702 (2008).
[5] C. Li, J. Yum, S. Moon, A. Herrmann, F. Eickemeyer, N. Pschirer, P. Erk, J. Schöneboom, K. Müllen, M. Grätzel, and M. Nazeeruddin, "An improved perylene sensitizer for solar cell applications," ChemSusChem **1**, 615–618 (2008).
[6] J.-L. Brédas, J. E. Norton, J. Cornil, and V. Coropceanu, "Molecular understanding of organic solar cells: The challenges," Acc. Chem. Res. **42**, 1691–1699 (2009).
[7] Y. Tanimura and S. Mukamel, "Optical stark spectroscopy of a brownian oscillator in intense fields," J. Phys. Soc. Jpn. **63**, 66–77 (1994).
[8] M. Tanaka and Y. Tanimura, "Quantum dissipative dynamics of electron transfer reaction system: Nonperturbative hierarchy equations approach," J. Phys. Soc. Jpn. **78**, 073802 (2009).
[9] X. Xie, A. Santana-Bonilla, and A. Troisi, "Nonlocal electron–phonon coupling in prototypical molecular semiconductors from first principles," J. Chem. Theory Comput. **14**, 3752–3762 (2018).
[10] A. A. Bakulin, A. Rao, V. G. Pavelyev, P. H. M. van Loosdrecht, M. S. Pshenichnikov, D. Niedzialek, J. Cornil, D. Beljonne, and R. H. Friend, "The role of driving energy and delocalized states for charge separation in organic semiconductors," Science **335**, 1340–1344 (2012).
[11] S. Gélinas, A. Rao, A. Kumar, S. L. Smith, A. W. Chin, J. Clark, T. S. van der Poll, G. C. Bazan, and R. H. Friend, "Ultrafast long-range charge separation in organic semiconductor photovoltaic diodes," Science **343**, 512–516 (2014).
[12] Y. Tanimura, "Stochastic liouville, langevin, fokker–planck, and master equation approaches to quantum dissipative systems," J. Phys. Soc. Jpn. **75**, 082001 (2006).